JOURNAL OF MATERIALS SCIENCE 28 (1993) 3329–3334

Vacancy concentration in strain ageing of substitutional f c c alloys

M. C. CHEN, L. H. CHEN, T. S. LUI
Department of Materials Engineering, National Cheng Kung University Tainan, Taiwan 70101

The relation between vacancy concentration, C_v and tensile plastic strain, ε, has been constantly expressed as $C_v \propto \varepsilon^m$. To take into account the grain-size effect, we have recently proposed that $C_v \propto \rho_m^\gamma$, where ρ_m is the mobile dislocation density. With the conventional expression that $\rho_m \propto \varepsilon^\beta d^{-n}$, where d is the average grain size, the strain and grain-size dependence of vacancy concentration appears to be $C_v \propto \varepsilon^{\beta\gamma} d^{-n\gamma}$. This equation has proved effective in rationalizing the onset strain, ε_c, and stress amplitude, $\Delta\sigma$, of flow instability associated with the Portevin–LeChatelier effect of substitutional f c c alloys, where ε_c and $\Delta\sigma$ are described by

$$\dot{\varepsilon} \propto \varepsilon_c^{\beta(1/2+\gamma)} d^{-n(1/2+\gamma)} T^{-1} \exp(-Q/kT)$$

and

$$\Delta\sigma \propto [\dot{\varepsilon}^{-1} \varepsilon^{\beta(1/2+\gamma)} d^{-n(1/2+\gamma)} T^{-1} \exp(-Q/kT)]^{2/3}$$

in which $\dot{\varepsilon}$, T, Q and k are the strain rate, temperature, Boltzmann constant and activation energy for solute migration, respectively. Using the same concept, we have obtained

$$\Delta\sigma_\gamma \propto [\varepsilon^{\beta\gamma} d^{-n\gamma} t_a T^{-1} \exp(-Q/kT)]^{2/3}$$

to rationalize the increment of stress drop, $\Delta\sigma_\gamma$, observed at the instant of reloading after a static ageing time of t_a. By adopting the above three equations, the strain-ageing data of two Al–Mg alloys in this study reveal that the vacancy concentration which is responsible for strain ageing is lower than the reported data from electrical resistivity measurements. This result is in agreement with the idea of migration of a vacancy–solute complex which has been proposed in the literature.

1. Introduction

Many experimental results [1] have shown that the increase of electrical resistivity of metals at low temperature, $\Delta\rho_e$, upon plastic strain, ε, can be interpreted as $\Delta\rho_e \propto \varepsilon^m$. By regarding $\Delta\rho_e$ as raised by vacancy generation during deformation, the vacancy concentration, C_v, can then be expressed empirically as [2–4]

$$C_v \propto \varepsilon^m \tag{1}$$

Because excess vacancies are produced by climb-related dislocation motions, one can also take C_v as proportional to ρ_m^γ empirically, where ρ_m is the mobile dislocation density. With the commonly adopted equation [5, 6] that

$$\rho_m \propto \varepsilon^\beta d^{-n} \tag{2}$$

where d is the average grain size, one then achieves

$$C_v \propto \varepsilon^{\beta\gamma} d^{-n\gamma} \tag{3}$$

The strain exponent, $\beta\gamma$, of Equation 3, is identical to m in Equation 1. However, Equation 3 also reveals a grain-size dependence which is neglected in Equation 1.

Equation 1 has been widely accepted to model the serrated flow associated with the Portevin–LeChatelier effect of substitutional f c c alloys [5, 7–18]; nevertheless, our recent analysis [19, 20] has shown that Equation 3 is more rational for the modelling. This analysis, which will be summarized in the next section, gives rise to two equations to rationalize the onset strain and stress amplitude of serration. Based on Equation 3, a third equation will also be derived in the present paper to interpret the stress drop which usually occurs on reloading after static strain ageing. The three equations will be adopted as a basis to characterize the vacancy concentration involved in strain ageing of substitutional f c c alloys. For the characterization, the data of two Al–Mg alloys will be reported and analysed.

2. Theoretical analysis

2.1. Onset strain and amplitude of serration

For substitutional f c c alloys under constant strain-rate tension, the critical strain at the onset of serration, ε_c, may decrease with increasing temperature [5, 9, 15, 21]; it may also decrease initially to a minimum and then increase with increasing temperature [22–24]. Despite this variation, there exists a region of decreasing ε_c with increasing temperature. In this temperature region, ε_c is normally observed to increase with increasing strain rate [5, 9, 10, 15] and grain size

[5, 15, 20, 25]. Meanwhile, the amplitude of serration, $\Delta\sigma$, increases with increasing strain and temperature [9, 21, 26]; it decreases with increasing grain size [9, 18, 27, 28] and strain rate [20, 29–31].

The famous Orowan equation

$$\dot{\varepsilon} \propto \rho_m \boldsymbol{b} V \tag{4}$$

where $\dot{\varepsilon}$, $\boldsymbol{b}$ and V are the strain rate, Burgers vector and average dislocation velocity, respectively, has been widely accepted as a primary equation to rationalize the above-described behaviour of ε_c and $\Delta\sigma$ [5, 7, 13–20, 32]. With L as the average pinning distance of a mobile dislocation, McCormick [11] has proposed the following equation to interpret the average dislocation velocity, V

$$V = L/t_a \tag{5}$$

where t_a is the total dynamic ageing time during dislocation motion and static ageing time while the dislocation is pinned. Normally, the dynamic ageing time can be neglected [11]. Therefore, t_a can be described by the following equation according to the static ageing model postulated by Cottrell and Bilby [33]

$$N(t_a) \propto C_0(Dt_a/kT)^{2/3} \tag{6}$$

where $N(t_a)$ is the number of solute atoms which diffuse to form a dislocation atmosphere during the static ageing time, t_a. C_0, D, k and T are the bulk average solute concentration, diffusion coefficient, Boltzmann constant and absolute temperature, respectively. By assuming that $N(t_a)$ at ε_c is a constant and the development of $\Delta\sigma$ is proportional to $N(t_a)$, substitution of Equations 2, 4 and 5 into Equation 6 leads to

$$\dot{\varepsilon}^{-1}\, \varepsilon_c^{\beta/2}\, d^{-n/2}\, T^{-1}\, D = \text{a constant} \tag{7}$$

and

$$\Delta\sigma \propto (\dot{\varepsilon}^{-1}\, \varepsilon^{\beta/2}\, d^{-n/2}\, T^{-1}\, D)^{2/3} \tag{8}$$

In deriving the above two equations, the average pinning distance, L, in Equation 5 has been taken as equal to $\rho_m^{-1/2}$ according to Mukherjee *et al.* [34].

For substitutional systems, the diffusion coefficient, D, in Equations 7 and 8 can be described as [8, 35–37]

$$D \propto C_v \exp(-Q/kT) \tag{9}$$

where Q is the activation energy for solute migration. With Equations 3 and 9, Equations 7 and 8 can be rewritten as

$$\dot{\varepsilon} \propto \varepsilon_c^{\beta(1/2+\gamma)}\, d^{-n(1/2+\gamma)}\, T^{-1} \exp(-Q/kT) \tag{10}$$

and

$$\Delta\sigma \propto (\dot{\varepsilon}^{-1}\, \varepsilon^{\beta(1/2+\gamma)}\, d^{-n(1/2+\gamma)}\, T^{-1} \exp(-Q/kT))^{2/3} \tag{11}$$

where the strain, ε, in Equation 3 has been taken as the critical strain, ε_c, in Equation 10.

In order to rationalize the grain-size effect, the above derivation of Equations 10 and 11 has used Equation 3 (i.e. $C_v \propto \varepsilon^{\beta\gamma} d^{-n\gamma}$) instead of Equation 1 (i.e. $C_v \propto \varepsilon^m$) for the description of vacancy concentration. In addition, the combination of Equation 4 (i.e. $\dot{\varepsilon} \propto \rho_m\, b\, V$) and Equation 5 (i.e. $V \propto L/t_a$) and other related equations gives rise to the strain-rate dependence of ε_c and $\Delta\sigma$ as revealed in Equations 10 and 11. In addition to Equation 5, the critical dislocation velocity, V_c, associated with maximum Cottrell atmosphere drag has also been frequently taken as the average dislocation velocity [5, 8–10, 15]. According to the Cottrell–Jaswon model [38], V_c can be expressed as

$$V_c \simeq 4kTD/A \tag{12}$$

where A is the position independent solute atom/edge dislocation interaction energy term.

By adopting Equation 1 for the vacancy concentration and Equation 5 or 12 for the average dislocation velocity, other kinetic equations besides Equation 10 can also be derived to interpret ε_c. However, much data [19] have indicated that Equation 10 is the most proper one among these equations to rationalize the grain-size effect. For the rationalization of $\Delta\sigma$, other kinetic equations besides Equation 11 can also be derived by adopting Equation 1 for the vacancy concentration. However, the data [20] have shown that only Equation 11 can rationalize the grain-size and strain-rate dependence of $\Delta\sigma$. Based on the above statement, and on the fact that both Equations 10 and 11 follow the same equations to describe C_v and V, Equations 10 and 11 should be appropriate to interpret ε_c and $\Delta\sigma$, respectively; C_v determined from these two equations should also be suited to represent the vacancy concentration involved in strain ageing. In the following sections, methods to determine C_v from Equations 10 and 11 will be shown. Also, C_v determined from the static strain-ageing experiments will be described.

2.2. Method of determining C_v from ε_c and $\Delta\sigma$

Under constant d and T, Equation 10 predicts that the slope of the ln $\dot{\varepsilon}$ versus ln ε_c plot is $\beta(1/2 + \gamma)$. Also, under constant $\Delta\sigma$, d and T, Equation 11 predicts that the slope of the ln $\dot{\varepsilon}$ versus ln ε plot equals $\beta(1/2 + \gamma)$. Because grain size is held constant and β can be determined separately from other experiments, $\beta\gamma$ in Equation 3 can then be obtained. Apparently, the vacancy concentration involved in strain ageing can thus be determined from the $\beta\gamma$ measurements.

2.3. Method to determine C_v from the static strain ageing

For substitutional fcc alloys such as Al–Mg [39, 40], Cu–Zn [41] and Cu–Sn [42] deformed in tension, a yield point usually occurs on restraining after static strain ageing. An analysis of this yield-point phenomenon has been proposed by Russell and Vela [42]. In their analysis, the stress drop, $\Delta\sigma_y$, from the yield point to the otherwise smooth flow curve was assumed to be proportional to the number of solute atoms which diffuse to a dislocation during a static ageing time, t_a according to Equation 6, i.e. $\Delta\sigma_y \propto N(t_a)$. Here, by adopting the assumption of Russell and Vela, substitution of Equations 3 and 9 into Equation 6, we

obtain

$$\Delta\sigma_\gamma \propto [\varepsilon^{\beta\gamma} d^{-n\gamma} t_a T^{-1} \exp(-Q/kT)]^{2/3} \quad (13)$$

Under constant d and T, Equation 13 predicts that the slope of the ln ε versus ln t_a plot is $-1/\beta\gamma$. Obviously, the $\beta\gamma$ in Equation 3 can also be obtained in this case. In the following sections the data of $\beta\gamma$ determined according to Equations 10, 11 and 13 will be reported for further analysis.

3. Experimental procedure

Al–1.9, 3.7 wt % Mg ingots (for detailed compositions see Table I), were used in this study. The ingots were heat treated for 3 days at 773 K and then extruded into round rods of 12 mm diameter. Tensile specimens with diameter 6 mm and gauge length 35 mm were machined from the extruded rods. The specimens were annealed at 773 K for 1 h and water-quenched prior to testing. The grain sizes of these two alloys, measured using the linear interception method, were 165 and 130 μm, respectively.

Al–3.7 wt % Mg was used in the tensile test. An Instron machine was used to conduct tensile tests at temperatures ranging from 210–273 K and strain rates ranging from 9.5×10^{-5}–1.05×10^{-2} s^{-1}. The load–time curves were plotted on a strip recorder equipped with zero suppression to extend the range of load for a better detection.

Under a constant strain rate of 5.2×10^{-4} s^{-1}, Al–1.9 wt % Mg was used in the static strain-ageing experiments. Four temperatures, ranging from 185–215K, were selected for the tests. The test procedure, shown schematically in Fig. 1, was the same as that described by Russell and Vela [42]. Namely, after a specific strain was reached, the specimens were aged for a fixed time, t_a, without load removal. Following the static strain ageing, the specimens were re-deformed to a second specific strain for the next ageing process which was a repeat of the previous one. This process was performed 15 times consecutively on each specimen. The stress drop, $\Delta\sigma_\gamma$, was then measured with respect to strain, temperature and ageing time.

4. Results

4.1. Measurement of ε_c and $\Delta\sigma$

A schematic representation of the typical stress–strain curve of Al–3.7 wt % Mg is shown in Fig. 2. The onset of serration is observed only after a critical strain, ε_c, is reached and the serration amplitude, $\Delta\sigma$, is observed to increase monotonically with strain before it becomes irregular. Only those $\Delta\sigma$ data in the monotonic region will be reported below.

TABLE I Chemical compositions of specimens used (wt %)

Alloy	Mg	Fe	Si	Mn	Ni	Al
Al–1.9 wt % Mg	1.90	0.10	0.059	0.01	0.018	Bal.
Al–3.7 wt % Mg	3.70	0.13	0.054	0.01	0.007	Bal.

Fig. 3 shows the ln $\dot{\varepsilon}$ versus ln ε_c plots for five test temperatures (i.e. 229, 239, 247, 257 and 273 K). The slopes of the linear curves in this figure are determined to be 2.0 ± 0.1.

Fig. 4 shows the ln $\dot{\varepsilon}$ versus ln ε plot for four test temperatures (i.e. 229, 239, 247 and 257 K), all with a constant $\Delta\sigma = 2$ MPa. The slopes of the linear curves in this figure were determined to be 1.8 ± 0.1.

4.2. Measurement of $\Delta\sigma_\gamma$

Typical results of the static strain-ageing experiments are given in Figs 5 and 6. In Fig. 5, the effect of strain and ageing time on the stress drop, $\Delta\sigma_\gamma$, under a constant temperature of 195 K is shown. $\Delta\sigma_\gamma$ is observed to increase with increasing strain and ageing time. Fig. 6 shows a plot of the data of stress drop versus strain for four test temperatures (i.e. 185, 195, 205 and 215 K), all with a fixed ageing time of 10 s. Except for

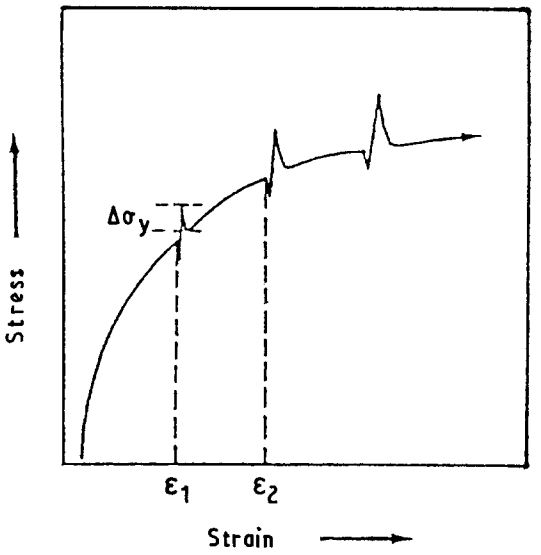

Figure 1 A schematic stress–strain curve showing the stress drop, $\Delta\sigma_\gamma$, on reloading steps after static strain ageing at specific strains.

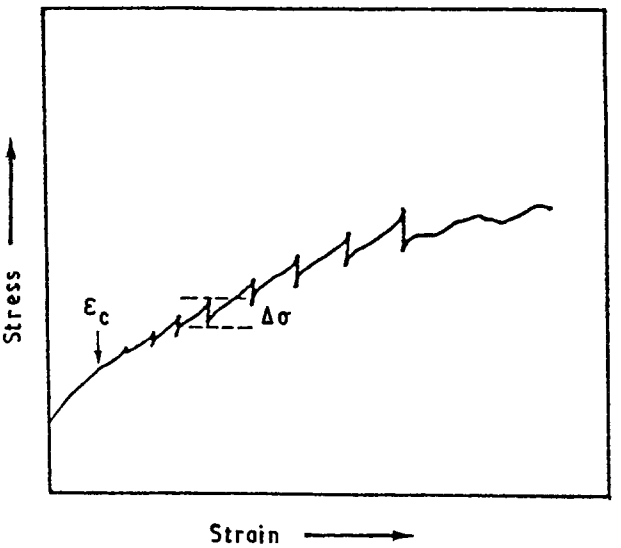

Figure 2 A schematic drawing of the typical flow curves obtained in this study, showing the critical strain, ε_c, at the onset of serration and the serration amplitude, $\Delta\sigma$.

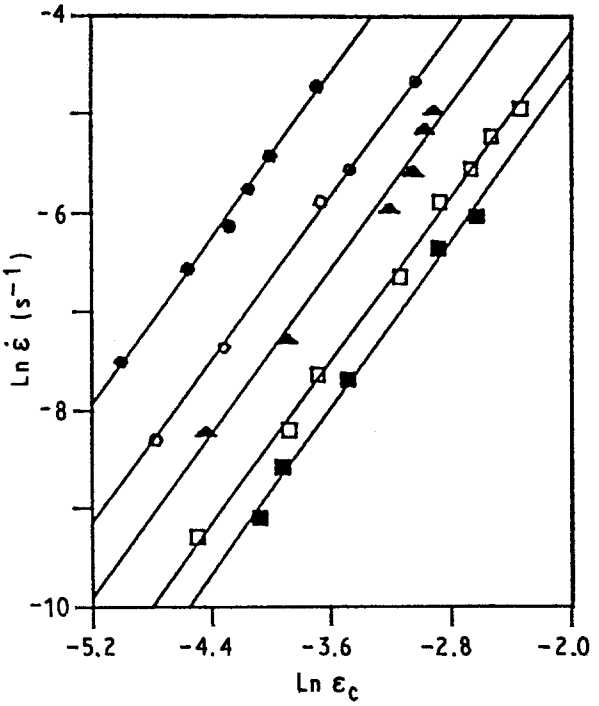

Figure 3 Logarithm plot of strain rate, $\dot{\varepsilon}$, versus critical strain, ε_c for various constant temperatures: (●) 273 K, (○) 257 K, (▲) 247 K, (□) 239 K, (■) 229 K.

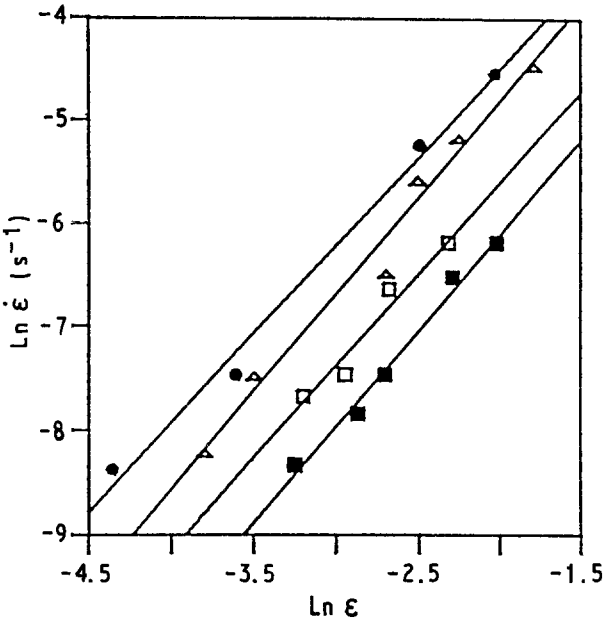

Figure 4 Logarithm plot of strain rate, $\dot{\varepsilon}$, versus plastic strain, ε. The data are associated with the same serration amplitude, i.e. $\Delta\sigma$ = 2 MPa. (●) 257 K, (△) 247 K, (□) 239 K, (■) 229 K.

those at 215 K at high strains, which are depicted by the dotted line in the figure, all the data reveal that the increase of $\Delta\sigma_\gamma$ with strain behaves monotonically. The high strain stress drop data at 215 K are accompanied by the appearance of serrated flow. To avoid complication, only those plots without serration are adopted for the analysis.

By choosing a constant $\Delta\sigma_\gamma$ of 1 MPa, Fig. 7 gives the respective ln ε versus ln t_a data for all the test temperatures. The slopes of the linear curves in this figure were found to be -0.48 ± 0.02.

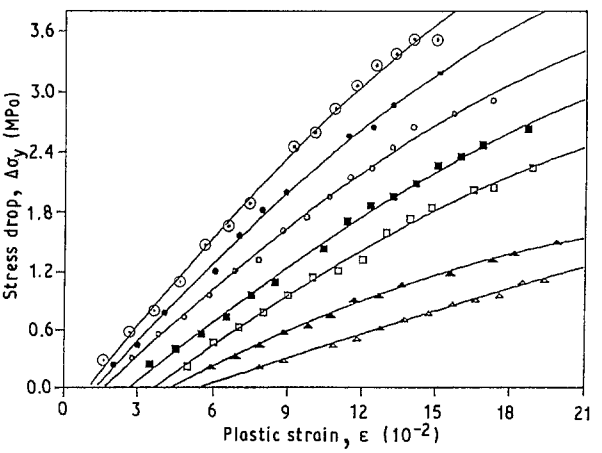

Figure 5 Effect of plastic strain and ageing time on the stress drop, $\Delta\sigma_\gamma$, T = 195 K. (——) No serrations, (– – –) serrations appear. t_a: (△) 5 s, (▲) 10 s, (□) 25 s, (■) 40 s, (○) 60 s, (●) 120 s, (⊙) 240 s.

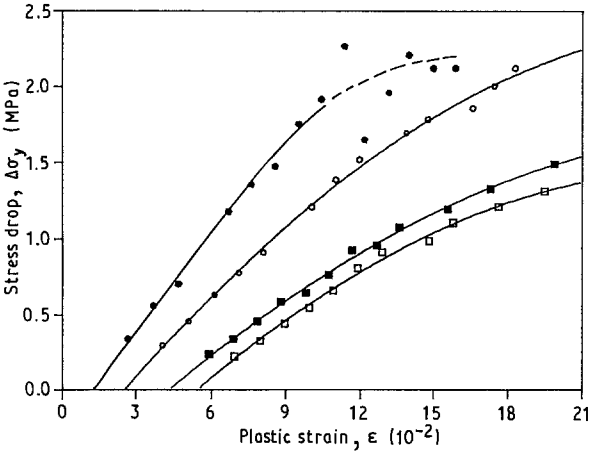

Figure 6 Stress drop versus plastic strain for the four test temperatures with ageing time, t_a = 10 s. (□) 185 K, (■) 195 K, (○) 205 K, (●) 215 K.

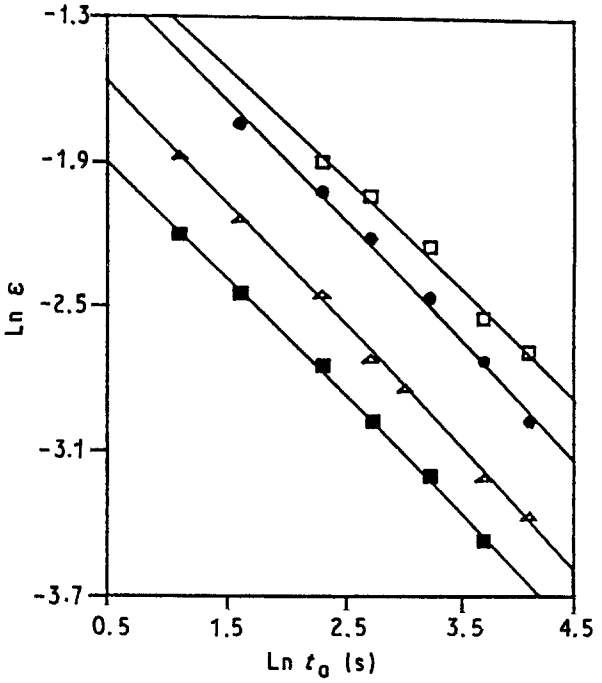

Figure 7 Logarithmic plot of plastic strain, ε, versus ageing time, t_a. The data are associated with the same stress drop, i.e. $\Delta\sigma_\gamma$ = 1 MPa. (□) 185 K, (●) 195 K, (△) 205 K, (■) 215 K.

5. Discussion

As stated previously, the vacancy concentration involved in strain ageing can be obtained from the determination of $\beta\gamma$ in Equation 3. However, the physical meaning of the obtained vacancy is ambiguous. To reveal the characteristic of the obtained vacancy, in the following, we will compare the $\beta\gamma$ with the m value determined according to Equation 1.

5.1. $\beta\gamma$ determined from ε_c

The results in Fig. 3 shows that the slope of ln $\dot{\varepsilon}$ versus ln ε_c plot is 2.0, which according to Equation 10 is equal to $\beta(1/2 + \gamma)$. The β values have been reported as 1.0 for aluminium [43] and copper [44], 1.05–1.08 for silver [45], 1.14–1.15 for Ag–6.3 wt % Al [46], 1.17 for Cu–5 wt % Sn [10] and 1.2 for many Cu–Zn alloys [47], all ranging from 1.0–1.2. On this basis, one may regard β as 1.0–1.2 for the Al–Mg in this study. Hence, $\beta\gamma$ in Equation 3 is then 1.4–1.5. No m value has been determined from Equation 1 for the binary Al–Mg alloy. However, m has been reported to be 1.0 for aluminium [1], 1.0–1.1 for Al–Mg–Si [12, 13] and 1.14 for Al–Mg–Mn [14]. Apparently, the most likely value of m for Al–Mg is in between 1.0 and 1.14. Comparing $\beta\gamma$ with m, reveals that $\beta\gamma$ is larger than m. Many data [19] have indeed shown that $\beta\gamma > m$. To check the coincidence of this result, $\beta\gamma$ obtained from the $\Delta\sigma$ and $\Delta\sigma_\gamma$ measurements, will be compared further with $m = 1.0$–1.14.

5.2. $\beta\gamma$ determined from $\Delta\sigma$

The results in Fig. 4 show the slope of ln $\dot{\varepsilon}$ versus ln ε plot is 1.8, which according to Equation 11 is equal to $\beta(1/2 + \gamma)$. By taking $\beta = 1.0$–1.2, $\beta\gamma$ is then 1.2–1.3 in this case. Again, the value of $\beta\gamma$ obtained is larger than $m = 1.0$–1.14.

5.3. $\beta\gamma$ determined from $\Delta\sigma_\gamma$

The results of Fig. 7 show that the slope of the ln ε versus ln t_a plot is -0.48 which, according to Equation 13, is equal to $-1/\beta\gamma$, i.e. $\beta\gamma = 2.08$. Obviously, this $\beta\gamma$ is also larger than $m = 1.0$–1.14.

5.4. The characteristic of vacancy involved in strain ageing

The above comparisons have shown that the $\beta\gamma$ values obtained from Equation 3 are all larger than the m values of Equation 1. Because the plastic strain is practically less than 1, the result $\beta\gamma > m$ reveals that the vacancy concentration which is responsible for strain ageing is lower compared to that determined from Equation 1. This phenomenon can be rationalized from the following consideration on the idea of vacancy–solute atom complex migration.

As pointed out by Cottrell [48], if a vacancy and a solute atom migrate together as a pair of vacancy–solute atom complex, the activation energy for such complex migration may be given as

$$E_v - E_b \qquad (14)$$

where E_v is the activation energy for a vacancy migration in pure metal and E_b is the binding energy between a vacancy and a solute atom. Brindly and Worthington [28] have shown that the activation energy obtained from the serrated flow in an Al–3 wt % Mg was 0.42 and 0.56 eV. By adopting Equation 14, because E_v in pure aluminium was reported as 0.75 eV [49, 50] and E_b for a vacancy and a magnesium atom was reported as 0.2 eV [51, 52], they can rationalize the obtained activation energy by 0.75–0.2 = 0.55 eV. Actually, many results [11, 15, 25, 53] have indeed attributed the activation energy associated with the serrated flow to the energy for a pair of vacancy–solute atom complex migration.

The above statement implies that the vacancy concentration which is responsible for strain ageing is determined by the effective combination number of the vacancy–solute atom complex. If the vacancy in the complex is considered to be that near the dislocation core region [19, 54], the meaning of $\beta\gamma > m$ could not be rationalized. However, as Johnson [55] pointed out, if a vacancy and a solute atom migrate together as a pair of vacancy–solute atom complex during diffusion, the complex can move in the lattice without the assistance of additional vacancies. According to this concept, the meaning of $\beta\gamma > m$ can be suitably rationalized.

6. Conclusions

1. Based on Equation 3 (i.e. $C_v \propto \varepsilon^{\beta\gamma} d^{-n\gamma}$), ε_c, $\Delta\sigma$ and $\Delta\sigma_\gamma$ can be expressed by Equations 10, 11 and 13, respectively. The vacancy concentration involved in strain ageing can then be determined from the measurement of $\beta\gamma$ through these three Equations.

2. From ε_c measurements, the slope of the ln $\dot{\varepsilon}$ versus ln ε_c plot is 2.0 which, according to Equation 10, results in $\beta\gamma = 1.4$–1.5; from $\Delta\sigma$ measurements, the slope of the ln $\dot{\varepsilon}$ versus ln ε plot is 1.8 which, according to Equation 11, results in $\beta\gamma = 1.2$–1.3; however from $\Delta\sigma_\gamma$ measurements, the slope of the ln ε versus ln t_a plot is -0.48 which, according to Equation 13, results in $\beta\gamma = 2.08$. $\beta\gamma$ values obtained in all the above three manners are larger than the m values determined from Equation 1.

3. $\beta\gamma > m$ reveals that the vacancy concentration involved in strain ageing is lower compared to that determined according to Equation 1. This phenomenon can be rationalized by the idea of vacancy–solute atom complex migration.

Acknowledgement

This work was supported by the Chinese National Science Council (Contract no. NSC 78-0405-E006-27, NSC 80-0405-E006-16 and NSC 81-0405-E006-548), for which we extend our thanks.

References

1. J. TAKAMURA, in "Physical Metallurgy", 2nd Edn, edited by R. W. Cahn (North-Holland, 1970) p. 894.
2. F. SEITZ, *Adv. Phys.* **1** (1952) 43.
3. H. G. VAN BUEREN, *Z. Metallkde* **46** (1955) 272.

4. *Idem, Acta Metall.* **3** (1955) 519.
5. W. CHARNOCK, *Phil. Mag.* **18** (1968) 89.
6. H. CONRAD and B. CHRIST, in "Recovery and Recrystallization of Metals", edited by L. Himmel (American Institute of Mining Engineers, NY, 1963) p. 124.
7. K. MUKHERJEE, C. D'ANTONIO and R. J. MACIAG, *Scripta Metall.* **4** (1970) 209.
8. A. H. COTTRELL, *Phil. Mag.* **44** (1953) 829.
9. B. RUSSELL, *ibid.* **8** (1963) 615.
10. R. K. HAM and D. JAFFREY, *ibid.* **15** (1967) 247.
11. P. G. McCORMICK, *Acta Metall.* **20** (1972) 351.
12. D. M. RILEY and P. G. McCORMICK, *ibid.* **25** (1977) 181.
13. P. G. McCORMICK, *ibid.* **22** (1974) 489.
14. J. A. TAYLOR and P. G. McCORMICK, *Mater. Sci. Engng* **21** (1975) 35.
15. S. MIURA, A. HAERIAN and S. HASHIMOTO, *J. Mater. Sci.* **22** (1987) 3446.
16. S. H. VAN DEN BRINK, A. VAN DEN BEUKEL and P. G. McCORMICK, *Phys. Status Solidi. (a)* **30** (1975) 469.
17. A. VAN DEN BEUKEL and U. F. KOCKS, *Acta. Metall.* **30** (1982) 1027.
18. R. ONODERA, H. ERA, T. ISHIBASH and M. SHIMIZU, *ibid.* **31** (1983) 1589.
19. M. C. CHEN, L. H. CHEN and T. S. LUI, *Acta Metall. Mater.* **40** (1992) 2433.
20. *Idem, Phil. Mag.*, submitted.
21. F. A. MOHAMED, K. L. MURTY and T. G. LANGDON, *Acta Metall.* **22** (1974) 325.
22. B. J. BRINDLEY and P. J. WORTHINGTON, *Metall. Rev.* **145** (1970) 101.
23. J. GUILLOT and J. GRILHE, *Acta Metall.* **20** (1972) 291.
24. R. W. HAYES, *Mater. Sci. Engng* **82** (1986) 85.
25. S. MIURA and H. YAMAUCHI, *Trans. Jpn Inst. Metals* **13** (1972) 82.
26. P. G. McCORMICK, *Acta Metall.* **19** (1971) 463.
27. *Idem, Phil. Mag.* **23** (1971) 949.
28. B. J. BRINDLEY and P. J. WORTHINGTON, *Acta Metall.* **17** (1969) 1357.
29. I. S. KIM and M. C. CHATURVEDI, *Mater. Sci. Engng* **37** (1979) 165.
30. E. PINK and A. GRINBERG, *Acta Metall.* **30** (1982) 2153.
31. *Idem, Mater. Sci. Engng* **51** (1981) 1.
32. L. P. KUBIN and Y. ESTRIN, *Acta Metall.* **38** (1990) 697.
33. A. H. COTTRELL and B. A. BILBY, *Proc. Phys. Soc.* **62** (1949) 49.
34. K. MUKHERJEE, C. D'ANTONIO, R. J. MACIAG and G. FISCHER, *J. Appl. Phys.* **39** (1968) 5434.
35. N. F. MOTT, *Phil. Mag.* 43 (1952) 1151.
36. *Idem, ibid.* **44** (1953) 187.
37. *Idem, ibid.* **44** (1953) 742.
38. A. H. COTTRELL and M. A. JASWON, *Proc. Roy. Soc.* **199** (1949) 1.
39. O. D. SHERBY, R. A. ANDERSON and J. E. DORN, *J. Inst. Metals* **3** (1951) 643.
40. A. R. C. WESTWOOD and T. BROOM, *Acta Metall.* **5** (1957) 249.
41. G. F. BOLLING, *Phil. Mag.* **4** (1959) 537.
42. B. RUSSELL and P. VELA, *ibid.* **8** (1963) 677.
43. J. G. RIDER and C. T. B. FOXON, *ibid.* **13** (1966) 289.
44. J. E. BAILEY, *ibid.* **8** (1963) 223.
45. J. E. BAILEY and P. B. HIRSCH, *ibid.* **5** (1960) 485.
46. S. HASHIMOTO and S. MIURA, *Mem. Fac. Engng Kyoto Univ.* **48** (1986).
47. J. N. LOMER and H. M. ROSENBERG, *Phil. Mag.* **4** (1959) 467.
48. A. H. COTTRELL, in "Vacancies and Other Point Defects in Metals and Alloys" (Institute of Metals 1958) p. 1.
49. R. O. SIMMONS and R. W. BALLUFFI, *Phys. Rev.* **117** (1960) 52.
50. J. BASS, *Phil. Mag.* **15** (1967) 717.
51. A. J. PERRY and K. M. ENTWISTLE, *J. Inst. Metals* **96** (1968) 344.
52. J. TAKAMURA, K. OKAZAKI and I. G. GREENFIELD, *J. Phys. Soc. Jpn* **18**, Suppl. III (1963) 78.
53. A. J. R. SOLER-GOMEZ and W. J. McG. TEGART, *Phil. Mag.* **20** (1969) 495.
54. M. C. CHEN, L. H. CHEN and T. S. LUI, *Scripta Metall.* **23** (1989) 655.
55. R. P. JOHNSON, *Phys. Rev.* **56** (1939) 814.

Received 14 September
and accepted 19 November 1992